Appendix

Paterka et al.

Contents:

Appendix Figure S1

Appendix Figure S2

Appendix Figure S3

Appendix Figure S4

Appendix Figure S5

Appendix Figure S6

Appendix Table S1

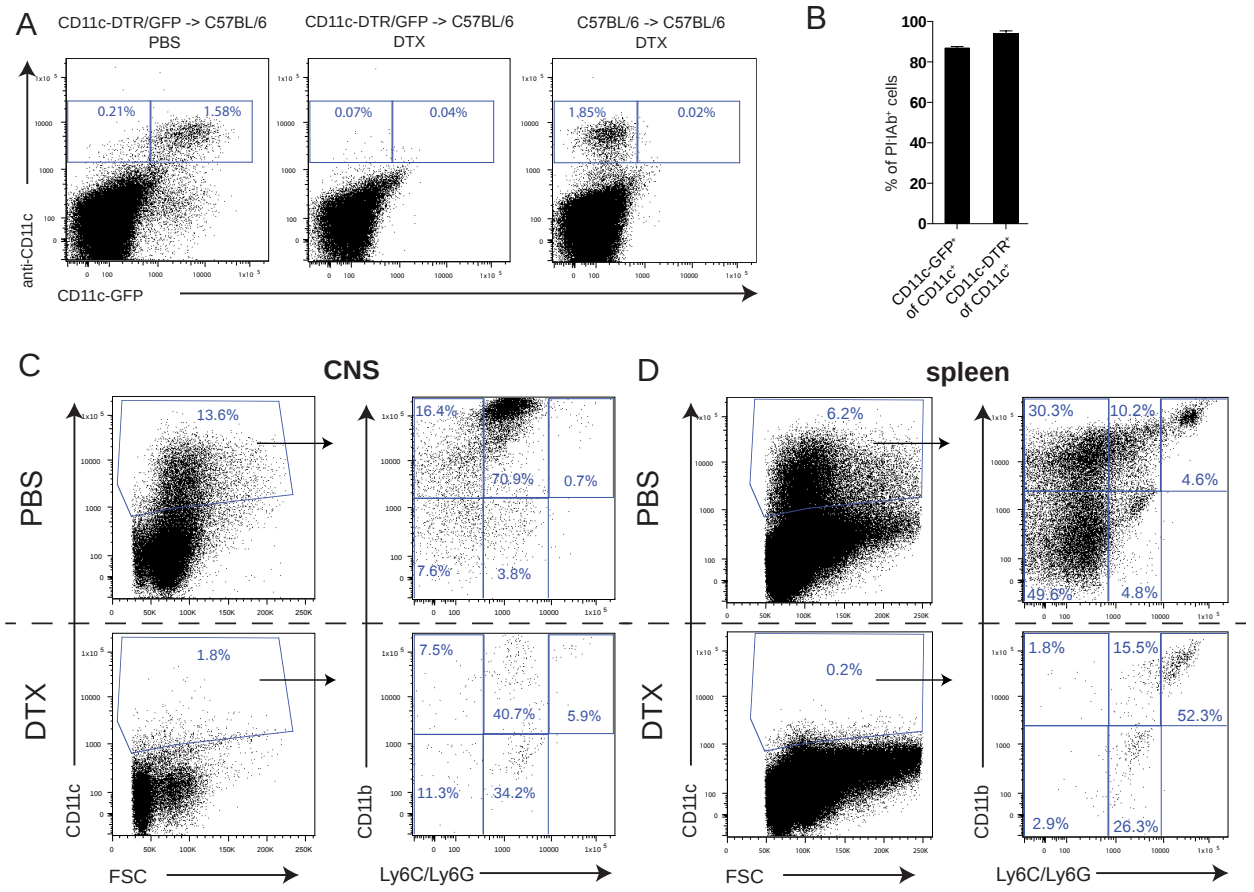

Characterization of CD11c engraftment and depletion by DTX in CD11c-DTR/GFP→C57BL/6.
(A) Chimerism of CD11c-DTR/GFP→C57BL/6 mice is shown by depiction of host-derived vs. donor-derived CD11c+ cells in the spleen of chimeric animals after at least six weeks of engraftment. >85% of CD11c$^+$ cells express also donor-derived CD11c-GFP. DTX application reveals that >93% of CD11c$^+$ cells can be depleted via the CD11c-restricted DTR. Control animals C57BL/6→C57BL/6, which were DTX treated, did not show alterations of the CD11c$^+$ cell numbers or proportions.
(B) Quantification of pooled data from two experiments for chimerism using GFP expression and DTX-mediated CD11c depletion efficiency.
(C) Depletion check of EAE animals (after 11 repetitive DTX applications every second day) in the chronic phase of active EAE (day 22). CNS cells from PBS-treated and DTX-treated EAE animals were stained for expression of cell markers and analyzed by flow cytometry. Cells were pre-gated on mononuclear MHCII-expressing cells.
DTX results show strong depletion, in particular of the Ly6C/G$^-$ CD11c$^+$ subset.
(D) Depletion check of EAE animals in the spleen; analogously to (C).
Representative FACS dotblots are shown for at least two independent experiments.

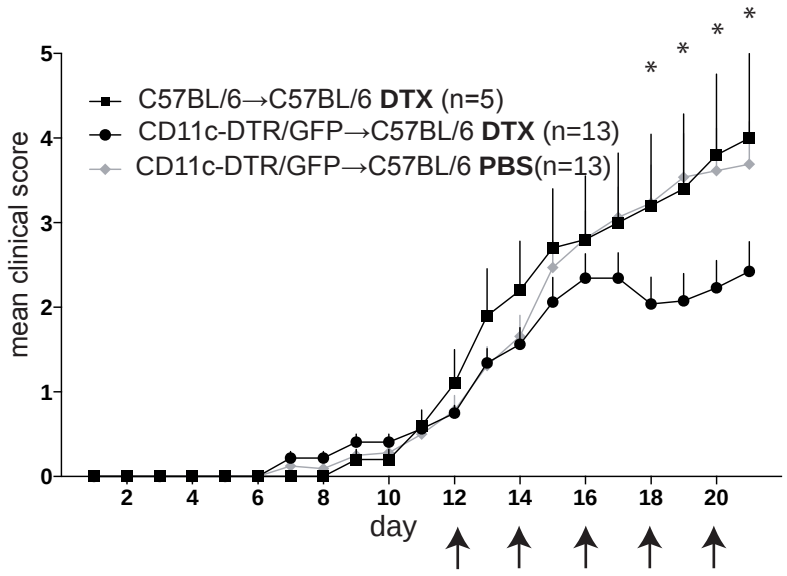

Peak depletion of CD11c$^+$ cells in active EAE in CD11c-DTR/GFP→C57BL/6. EAE was induced by subcutaneous immunization of CFA/MOG_{35-55} and pertussis toxin on d0 and d1. In order to investigate the effect of CD11c$^+$ depletion after onset of EAE (effector phase), DTX treatment was started after animals reached a mean score of 1. Controls were C57BL/6→C57BL/6 treated with DTX and CD11c-DTR/GFP→C57BL/6 treated with PBS. Statistical analysis by the Mann-Whitney-U Test for DTX- vs. PBS-treated CD11c-DTR/GFP→C57BL/6; * $p < 0.05$.

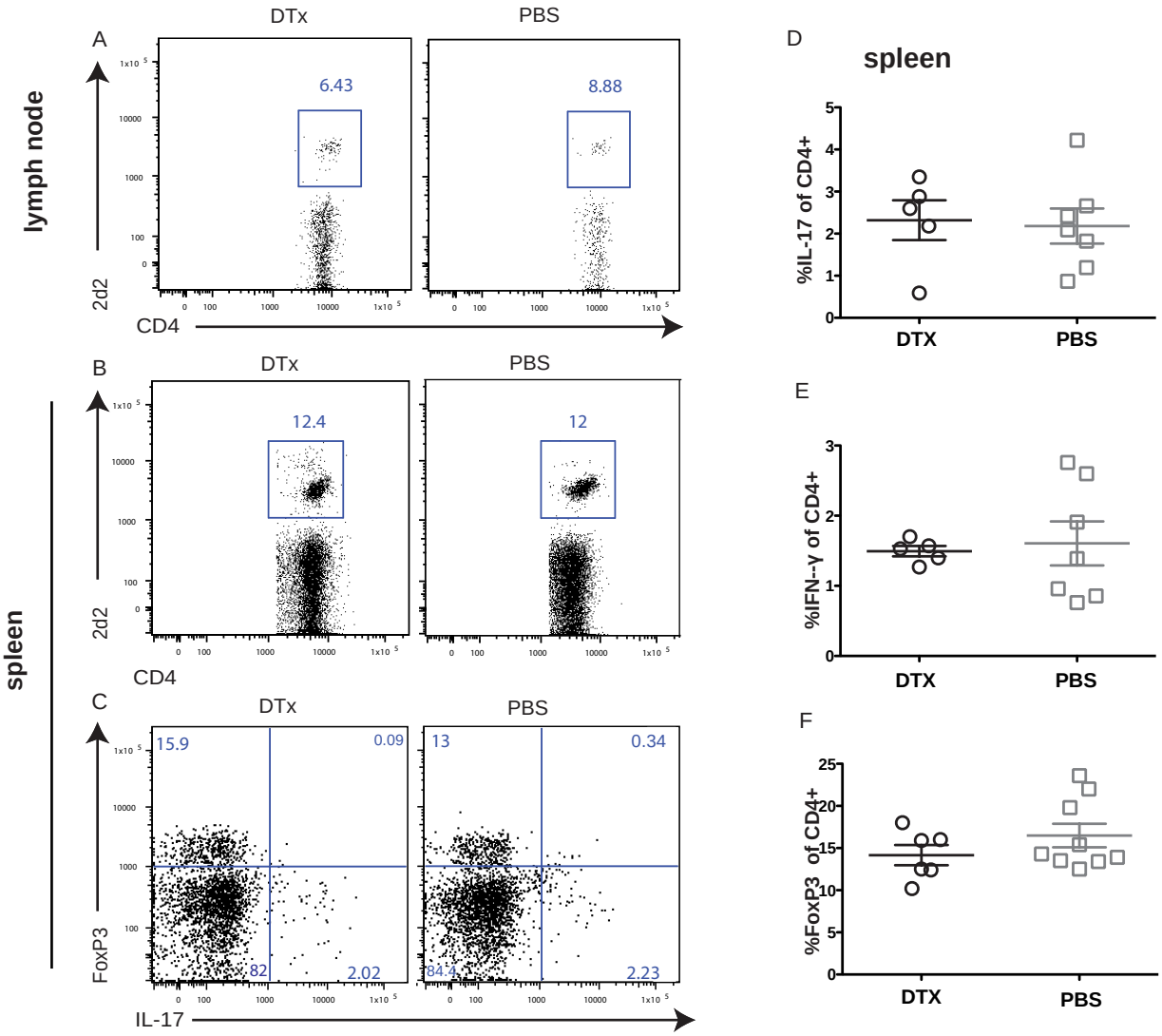

In adoptive transfer EAE CD11c depletion has no effect on survival of T cells in secondary lymphoid organs.

(A) 2-3 days after onset of clinical signs, there was no difference between 2d2.tdRFP Th17 cells in numbers in lymph nodes of DC-depleted and non-depleted mice.

(B) Similarly as in lymph nodes, numbers of 2d2.tdRFP Th17 did not differ in DC-less and DC-harboring mice in the spleen.

(C) FACS analysis of anti-CD3/anti-CD28 stimulated spleen cells showed neither differences for the pro-inflammatory cytokine IL-17 nor for FoxP3 expression of CD4+ T cells.

(D)-(F) Quantification of representative data as shown in (C).

A

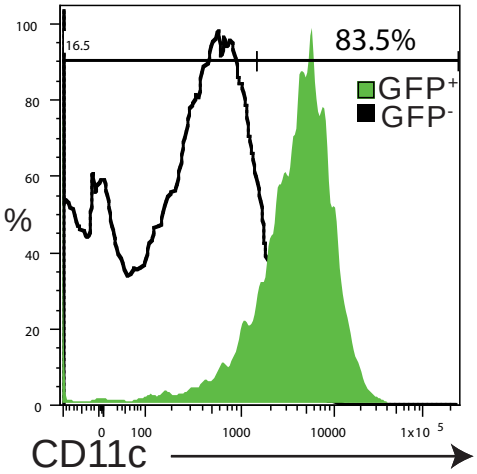

B

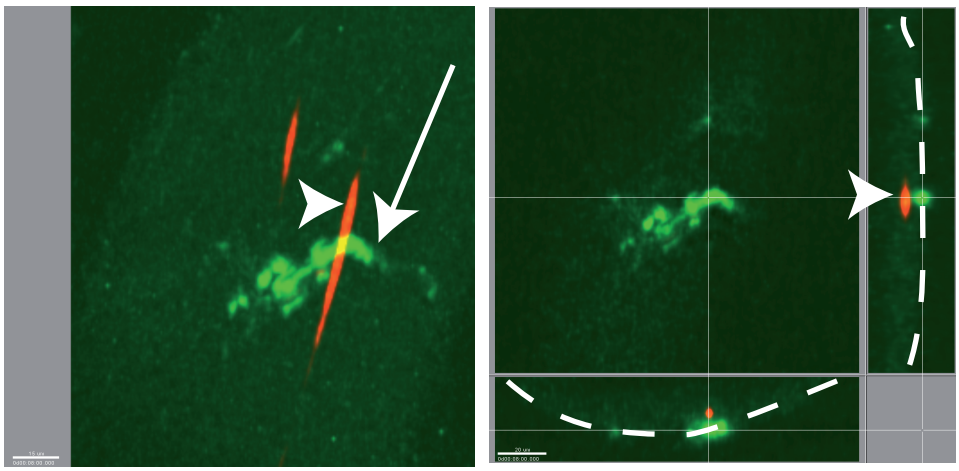

Ex vivo CD11c-GFP expression in EAE CNS tissue correlates with CD11c protein expression.
Adoptive transfer EAE was induced in CD11cDTR/GFP mice by 2d2.tdRFP Th17.
(A) Mononuclear cells isolated from EAE affected mice showed strong correlation of CD11c protein expression in GFP-positive cells.
(B) Before onset of the disease only rare numbers of GFP-positive cells can be visualized in the brainstem by TPLSM (see also Fig. 1). CD11c-GFP cells are located near venules (arrow, dotted line marks vessel surface). 2d2.tdRFP cells are passing trough the blood stream before onset (arrowhead).

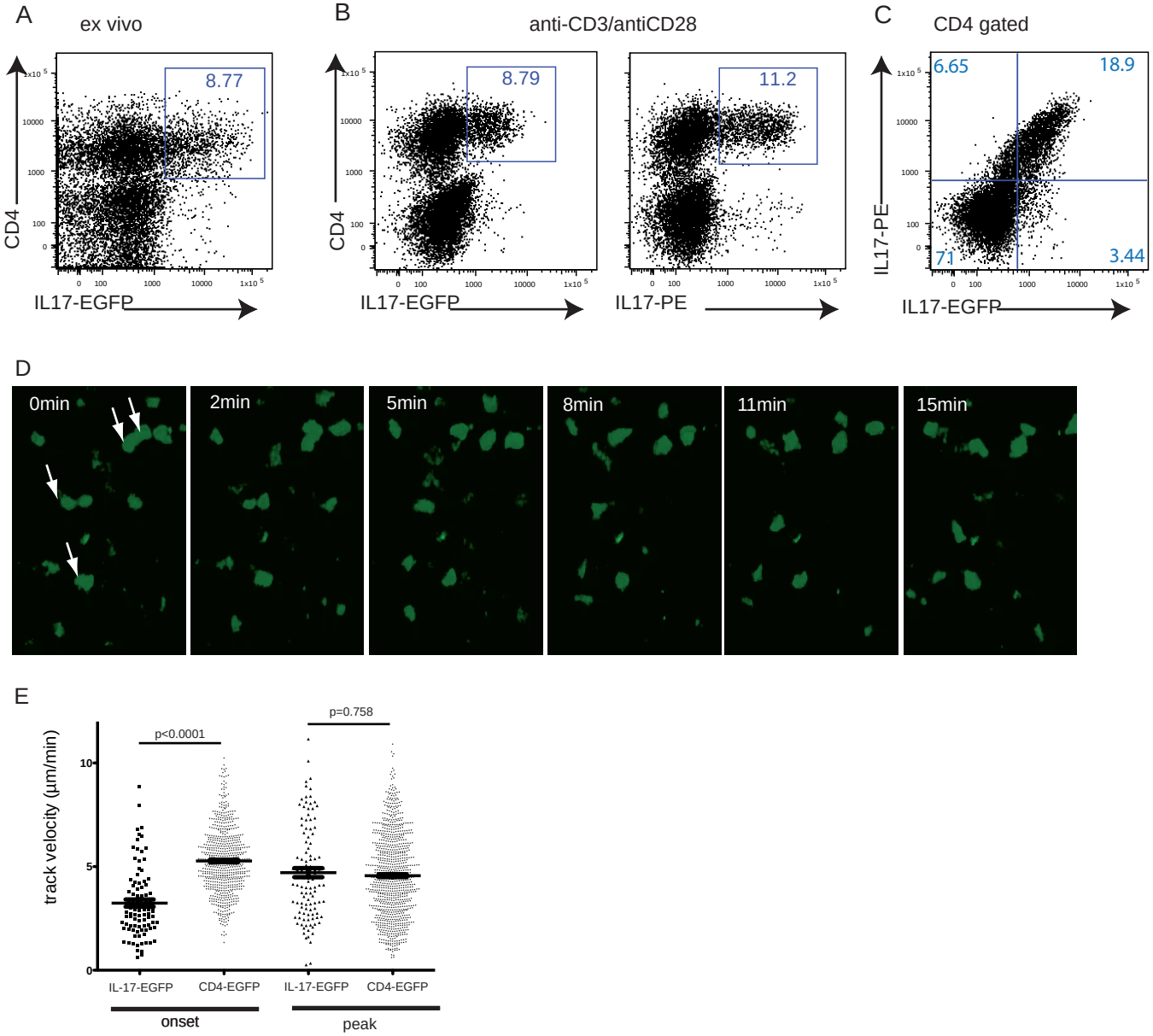

Ex vivo IL-17A-EGFP expression in EAE CNS tissue correlates with IL-17A protein expression.
(A) Mononuclear cells isolated from (active) EAE affected B6.*IL17A*-EGFP mice (pooled CNS tissue from 2 animals; onset of the disease, score 2, clinical signs for 2 days) consisted of considerable numbers of IL-17-EGFP expressing CD4+ T cells (gated on Propidium iodide (PI)-negative lymphocytes).
(B) The EGFP expression rate closely correlated with the IL-17 protein production capacity as shown by staining against IL-17 protein upon stimulation by anti-CD3/anti-CD28.
(C) EGFP expression and protein staining overlap closely in CD4+ T cells (gated on CD4+ T cells).
(D) Intravital TPLSM in the brainstem of living anaesthetized IL-17-EGFP mice with active EAE revealed efficient EGFP expression for intravital microscopy. IL-17A-EGFP^{hi} cells show locally restricted migratory behavior (arrows).
(E) Cell track analysis (mean track velocity) of IL-17-EGFP cells vs. CD4+ EGFP cells in active EAE in the onset (d1-2) and peak (>d2) of the disease

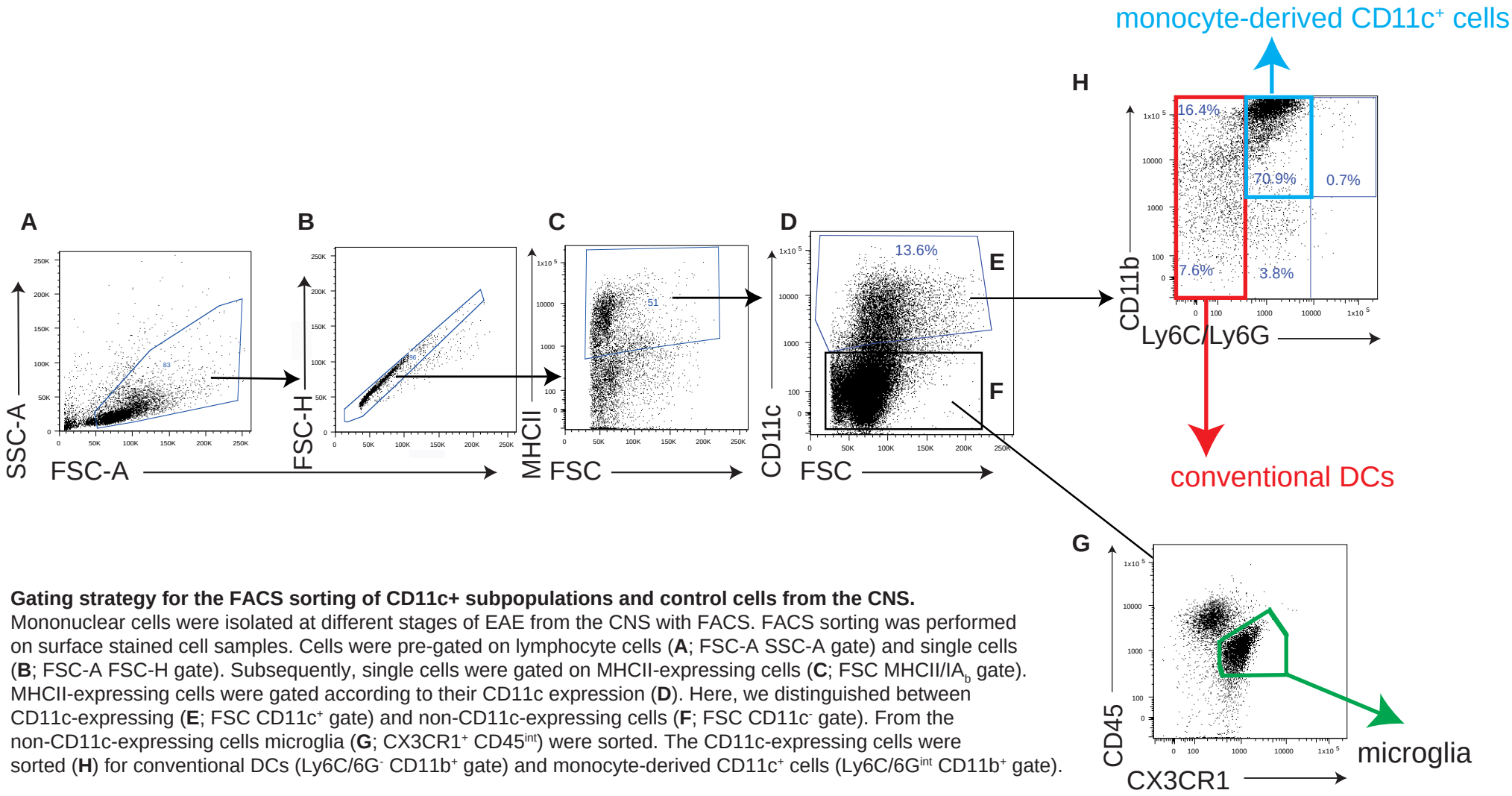

Gating strategy for the FACS sorting of CD11c+ subpopulations and control cells from the CNS.
Mononuclear cells were isolated at different stages of EAE from the CNS with FACS. FACS sorting was performed on surface stained cell samples. Cells were pre-gated on lymphocyte cells (**A**; FSC-A SSC-A gate) and single cells (**B**; FSC-A FSC-H gate). Subsequently, single cells were gated on MHCII-expressing cells (**C**; FSC MHCII/IA_b gate). MHCII-expressing cells were gated according to their CD11c expression (**D**). Here, we distinguished between CD11c-expressing (**E**; FSC $CD11c^+$ gate) and non-CD11c-expressing cells (**F**; FSC $CD11c^-$ gate). From the non-CD11c-expressing cells microglia (**G**; $CX3CR1^+$ $CD45^{int}$) were sorted. The CD11c-expressing cells were sorted (**H**) for conventional DCs ($Ly6C/6G^-$ $CD11b^+$ gate) and monocyte-derived $CD11c^+$ cells ($Ly6C/6G^{int}$ $CD11b^+$ gate).

Clinical EAE upon passive transfer of 2d2.tdRFP Th17 cells (*see* **Fig. 2A**)

Mice			Clinical EAE			
	Treatment	n	**Incidence**	**Mean day of onset***	**Mean maximal score***	**Mean score[§]**
CD11cDTR→ C57BL/6	DTX	13	30.78%	29.25 ± 0.96	1.25 ± 0.5	0.05 ± 0.03
CD11cDTR→ C57BL/6	PBS	11	63.36%	24 ± 1.41	4.14 ± 0.9	0.51 ± 0.45

[§] includes all animals in the experiment

* includes only diseased animals